Multiscale Atmospheric Simulations over a Complex Terrain: Surface Variability and Land-Atmosphere Exchange

Charles Talbot, Elie Bou-Zeid and Jim Smith

Department of Civil and Environmental Engineering, Princeton University, Princeton NJ

Abstract:

This study highlights the impacts of the surface variability on Land-Atmosphere interactions using multi-scale atmospheric simulations with the Weather Research and Forecasting model capacities, coupled with NOAH land surface model and Kusaka et al. (2001) urban canopy model. The 30-m resolution numerical datasets for land-use and topography are respectively given by National Land-Cover Dataset (NLCD 2001) and Shuttle Radar Topography Mission (SRTM). The finest simulation is performed with a grid size of 50 m, to study near-surface atmospheric dynamics and surface energy budget for a perfectly cloud-free day: atmospheric pressure changed within the day from 1015 hPa to 1019 hPa, recorded 2-m temperatures varied from 10°C to 27°C, specific humidity varied between 6 and 8 g/kg, while wind speed remained below a velocity of 9 m/s.

Despite identical initial and boundary conditions (soil type, land use and soil moisture) as well as identical mesoscale meteorological forcing and radiative forcing, the real-case large eddy simulation indicates a large discrepancy of computed surface fluxes within the same land-use type. These discrepancies of surface fluxes, as large as 140W/m² variation for water bodies, can be directly attributed to the surface variability around each grid cell imputed to the heterogeneity of land use and topography of this complex terrain.

Introduction:

Surface fluxes play a key role in surface-atmosphere interactions. These interactions between the heterogeneous land-surface and the atmosphere are conditioning the atmospheric boundary layer depth (Strunin et al. 2004), which in returns influences the near-surface atmospheric dynamics and mean surface fluxes (Courault et al. 2005).

Local ABL models nested inside mesoscale models allow bridging the gap between mesoscale forcing and small scales physics and more particularly, in the framework of land-surface atmosphere interactions, coupling online land-surface models with LES, whose boundaries are forced by mesoscale meteorological systems. WRF possesses a variety of land-surface models but NOAH land surface model (Chen F. and Dudhia J., 2001) was chosen since it is coupled with Kusaka et al. (2001) urban canopy model.

NOAH land-surface model computes surface and ground fluxes for the dominant land-use type of a grid cell. This dominant land-cover will thus exclude all heterogeneities within the grid cell area. The coarser the model grid resolution, the more inappropriate the results may be for a local computation of the surface energy balance. In order to capture, at mesoscales, multiple surface features induced by heterogeneities some distinctive approaches (e.g. Claussen 1991) propose to take into account effective values of surface properties such as roughness length and surface temperature. These approaches yield a statistical description of heterogeneities in mesoscale models. Our approach here is different since we are actually computing near-surface dynamics at small scale, by means of large eddy simulations, and we can thus estimate the impacts of surface heterogeneities on flow dynamics and the resulting surface fluxes. These results can be later aggregated into regional scale formulations for averaged fluxes similar to the ones proposed by for example by Bou-Zeid *et al.* (2007).

The next section is a brief explanation of the model setup and the adaptation of numerical datasets that will match the smallest scale of our large eddy simulation model. The results are then presented is section 3 before leading to the conclusions.

Model set-up:

Multi-scale atmospheric simulations are a combination of nested atmospheric models. The 3 first “weather type” (mesoscale) models (D1, D2 and D3) have resolutions of 12.15 km, 4.05 km and 1.35 km. The largest area covers the North-East coast of the USA and the smallest is the center region of the state of New Jersey (see maps on Figure 1). The numbers of grid points are 90x80 horizontally and 109 vertical levels for all the mesoscale simulations. The ABL dynamics in these models are simulated with the Yonsei University PBL scheme (Noh et al., 2003; Hong et al. 2006).

The 3 LES models (D4, D5 and D6) have resolutions of 450 m, 150m and finally 50 m. This gives domains areas ranging from 40×40 km for the largest LES model, to 5×5 km for the finest model centered over Princeton, New Jersey. The large amount of vertical grid points allows a rather fine resolution near the ground, 12 m height above ground level on average. All models have 44 verticals levels in the first thousand and two hundreds meters.

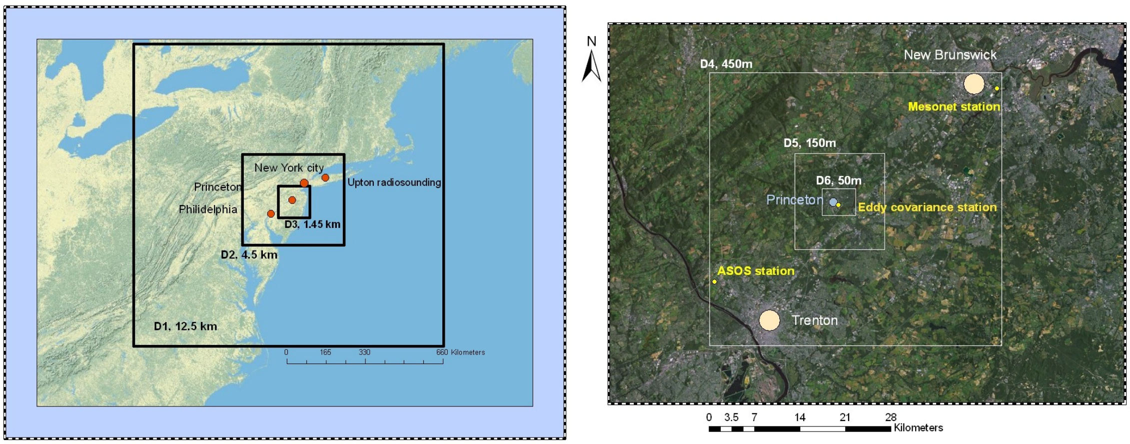

Figure 1. (a) Map of the North-East coast of US: the three nested mesoscale domain boundaries are represented by the black rectangles. (b) Google earth picture: the 3 nested LES model boundaries are represented by 3 white rectangles. The simulation names (D1 to D6) are followed by the horizontal grid resolution.

The geographical data for the land-use and topography for the non-LES models come from the standard USGS dataset and have a resolution of 2 arc minute for first domain and 30-arc second resolution for models 2 and 3 (respectively 4.05 km and 1.35 km). All static fields have been remapped for the 3 LES models. Topography has been redirected to the 1-arc second resolution (30 m) Shuttle Radar Topography Mission dataset (SRTM) (Rabus et al. 2003, Farr et al. 2007). http://www2.jpl.nasa.gov/srtm/. The land-use dataset, used by the NOAH land-surface model, is adapted from the National Land Cover Dataset (NLCD 2001: Homer et al., 2004), which has been established by the Multi-Resolution Land Characteristics consortium (MRLC, http://www.mrlc.gov/about.php), resulting in a 1-arc second resolution (30 m) dataset (Figure 2).

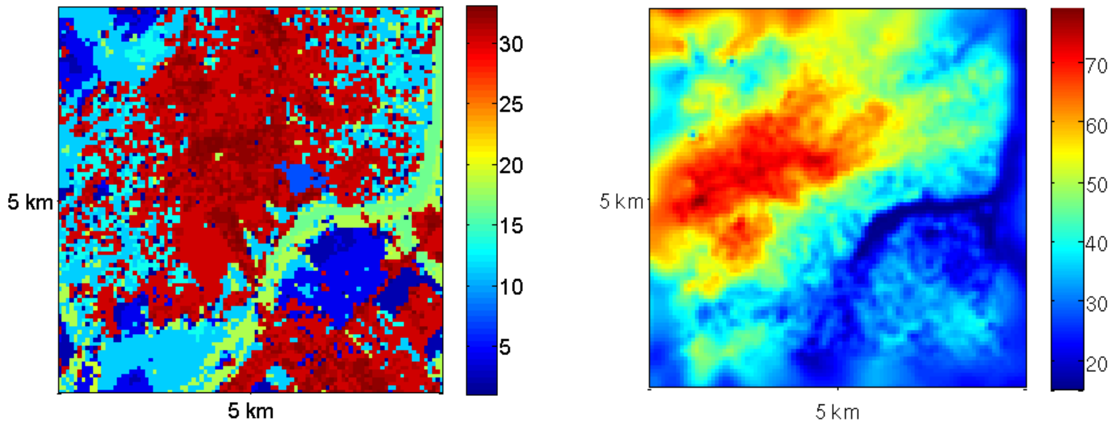

Figure 2. These two maps represent static fields in the finest resolution (50 m) model over Princeton Township: (a) land-use types from National Land Cover Dataset 2001. The red colors represent urban areas, while forests are in light blue, crops in dark blue, and lake in green. (b) Topography map from Shuttle Radar Topography Mission data in meters: the highest location is culminating at 80m (red) and lowest is in dark blue indicating the lake elevation.

The urban canopy model (UCM) has been adapted for four urban categories and remapped in WRF land cover static files. These categories directly originate from the NLCD 2001, 30-m resolution dataset. A new urban category ("urban open space") is added to WRF standard 3-urban categories. A summary of models description can be found in Appendix A.

The rather large amount of vertical grid points, 109, allows a fine vertical resolution near the ground, where atmosphere-land surface interactions occur.

Meteorological input data are taken from North American Regional Reanalysis ETA model products.

Results:

Simulation results for the whole diurnal cycle of September 24th, 2007 indicate a cloud-free day over Princeton, in accordance with our local radiometer measurements. Time series in the simulation domains were recorded at different locations and indicate similar levels of downward shortwave and longwave radiation for each position (not shown here), confirming the absence of clouds.

Figure 3 represents the deviation of a surface variable (soil moisture, sensible and latent heat flux), at each grid point of domain 6, from its spatial average over the whole domain; the results are also averaged in time over one diurnal cycle (e.g. $\langle H\rangle_t - \langle H\rangle_{t,x,y}$ where the subscripts denote averaging in a given direction). The results highlight the various contributions of each land use. One clearly sees the dominant contribution of the lake and urban areas in sensible heat flux (Figure 3b). Carnegie Lake appears largely as the major source of evaporation with 80 W/m² above the domain–averaged LE. In the mean time, a large deficit of evaporation can be depicted in urban areas.

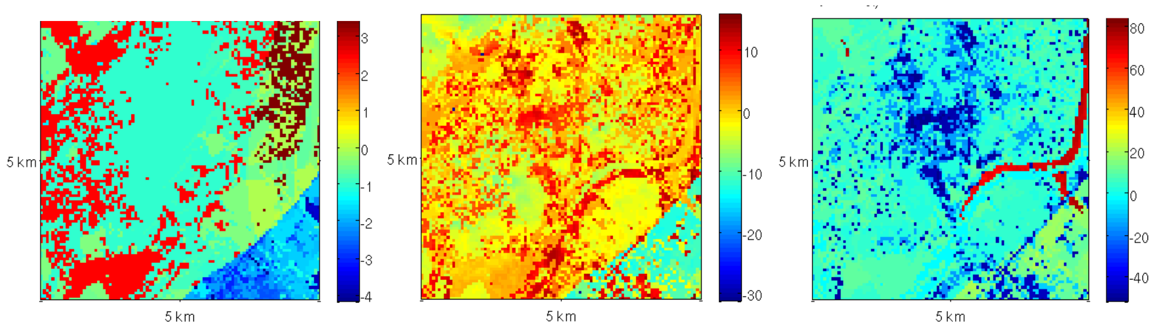

(a) (b) (c)

Figure 3. Difference between a time-averaged quantity for a specific grid cell and space-time averages of the same quantity for the whole domain: for (a) soil moisture, (b) sensible heat flux and (c) latent heat flux.

The impact of the soil type is clearly visible in the mean intensity plots of surface fluxes and generates a strong horizontal gradient in mean quantities. A least important gradient of these same quantities is also generated with initial conditions of soil moisture. This gradient of surface fluxes may favor secondary circulations in the near-surface dynamics (Courault et al. 2005). This is probably an artifact of NOAH LSM. This feature is probably attenuated in reality.

This observation led us to another type of analysis. Figure 4 represents the 5 different zones of domain 6 in which initial conditions of soil moisture and soil type are identical. For example, the dark blue area represents a zone where the soil type is silt loam and initial soil moisture is 0.018 g/m3. Mean and variant values of surface fluxes were analyzed within these zones to avoid influences from different initial/boundary conditions.

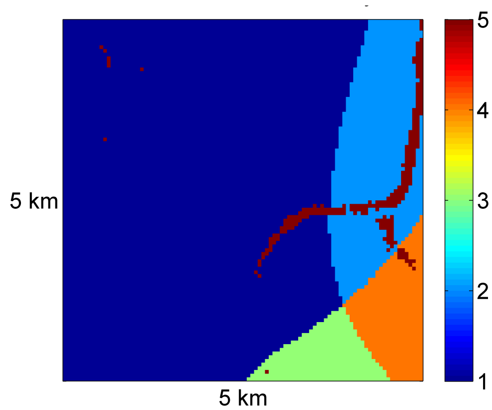

Figure 4. Different zones of identical initial and boundary conditions in terms of soil moisture and soil type.

Figure 5 represents the difference between the minimum and maximal value of sensible heat flux within area 1 (dark blue area) and for 4 different land-use types (low intensity urban, wooded wetland, lake and dry-land/cropland and pasture). One can observe that even within identical radiative forcing, initial and boundary soil moisture conditions, a large difference in the surface fluxes is obtained for the same land-use type. With this conditional sampling to control for other various sources of variability, the observed spatial variability can be linked to the land-use heterogeneity which then results in variability in the wind speed, turbulence, and air temperature and relative humidity over the simulation domain.

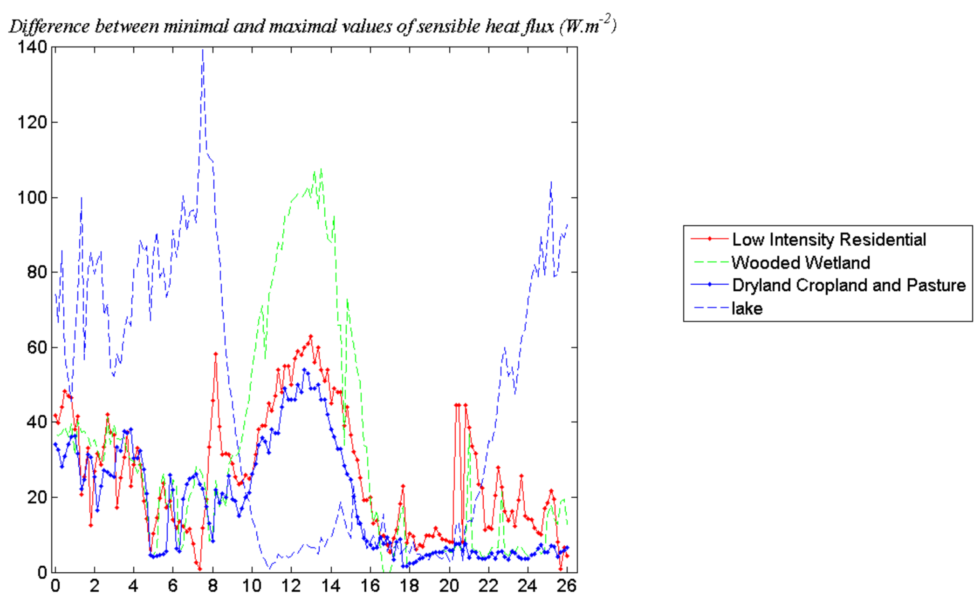

Figure 5. The difference between the lowest and highest sensible heat fluxes over an individual land-use type, as a function of time of day within area 1.

Conclusions:

The WRF model, coupled with NOAH LSM and Kusaka et al. UCM, were used for multi-scale atmospheric simulations, from 12.15-km down to 50-m horizontal resolution, and over a heterogeneous and complex terrain under real meteorological forcing. SRTM and NLCD 2001 datasets were implemented in the static fields to have a matching resolution for land use and topography. A fourth urban category was added to WRF to match NLCD urban categories.

A full diurnal cycle of a cloud free day was simulated and near-surface dynamics were analyzed. A large variability in surface fluxes was observed over locations with identical land-use type, radiative forcing, soil type and initial soil moisture condition. This variability was linked to the land-use heterogeneity which then results in variability in the wind speed, turbulence, and air temperature and relative humidity over the simulation domain.

Acknowledgment:

The work is supported by the High Meadows Sustainability Fund of Princeton University and by the Mid-Infrared Technology for Health and the Environment (MIRTHE) NSF center at Princeton University. Numerical simulations were done under CISL project #36861019 on NCAR/UCAR supercomputers.

Appendix A:

Table: Six nested models used for the multiscale atmospheric simulations

Model type	**dx,dy**	**grid points**	**time steps**
D1 Mesoscale (YSU PBL)	12150 m	91x82x109	72s
D2 Mesoscale (YSU PBL)	4050 m	91x82x109	24s
D3 Mesoscale (YSU PBL)	1350 m	91x82x109	8s
D4 Microscale (LES)	450 m	91x82x109	4/3s
D5 Microscale (LES)	150 m	91x82x109	2/9s
D6 Microscale (LES)	50 m	100x100x109	2/27 s

References:

Bou-Zeid, E., Parlange, M., and Meneveau C., 2007: On the Parameterization of Surface Roughness at Regional Scales. J. Atm. Sci., 64, pp 216-227.

Chen F. and Dudhia J., 2001: Coupling an Advanced Land Surface-Hydrology Model with the Penn State-NCAR MM5 Modeling System. Part I: Model Implementation and Sensitivity, Mon. Weather Rev., Vol. 129, no. 4, pp. 569-585.

Claussen M., 1991: Estimation of Areally-Averaged Surface Fluxes. Boundary-layer Meteorology, 54(4), 387-410.

Courault D., P. Drobinski, Y. Brunet, P. Lacarrère and C. Talbot, 2007: “Impact of surface heterogeneity on a buoyancy-driven convective boundary-layer in light winds”, Boundary- Layer Meteorology, DOI 10.1007/s10546-007-9172-y.

Farr, T. G., Rosen, P. A., Caro, E., Crippen, R., Duren, R., Hensley, S., Kobrick, M., Paller, M., Rodriguez, E., Roth, L., Seal, D., Shaffer, S., Shimada, J., Umland, J., Werner, M., Oskin, M., Burbank, D., and Alsdorf, D., 2007: The Shuttle Radar Topography Mission. Rev. Geophys., 45, RG2004, doi:10.1029/2005RG000183.

Homer, C., Huang, C., Yang, L., Wylie, B., Coan, M.,2004: Development of a 2001 National Land-Cover Database for the United States, Photogrammetric Engineering and Remote Sensing, 70, 7, 829-840.

Hong, S.Y., Y. Noh, and J. Dudhia, 2006: A new vertical diffusion package with an expliticit treatment of entrainment processes. Mon. Wea. Rev., 134, 2318-2341.

Kusaka, H.; Kondo, H.; Kikegawa, Y.; Kimura, F., 2001: A Simple Single-Layer Urban Canopy Model For Atmospheric Models: Comparison With Multi-Layer And Slab Models. Bound.-Layer Meteorol., Vol. 101, no. 3, pp. 329-358.

Noh, Y., Cheon, W. G., Hong, S.Y., and Raasch, S., 2003: Improvements of the K-profile for the planetary boundary layer based on large eddy simulation data. Bound.-Layer Meteor., 107, 401-427.

Rabus, B., M. Eineder, A. Roth, R. Bamler, 2003: The shuttle radar topography mission- a new class of digital elevation models acquired by spaceborne radar, Photogramm. Rem. Sens., v. 57, p. 241-262.

Strunin, M.A., Hiyama, T., Asanuma, J., and Ohata, T.: 2004, “Aircraft observations of the development of thermal internal boundary layers and scaling of the convective boundary layer over non-homogeneous land surfaces”, Boundary-Layer Meteorol., 111 (3), 491-522.